Hepatocyte NAD(P)H oxidases as an endogenous source of reactive oxygen species during hepatitis C virus infection

Nabora Soledad Reyes de Mochel[1], **Scott Seronello**[1], **Shelley Hsiuying Wang**[1], **Chieri Ito**[1], **Jasper Xi Zheng**[1], **T. Jake Liang**[2], **J. David Lambeth**[3], and **Jinah Choi**[1,*]

[1]School of Natural Sciences, University of California, Merced, CA

[2]Liver Diseases Branch, National Institute of Diabetes and Digestive and Kidney Diseases, National Institutes of Health, Bethesda, MD

[3]Emory University, Atlanta, GA

Abstract

Oxidative stress has been identified as a key mechanism of hepatitis C virus (HCV)-induced pathogenesis. Studies suggest that HCV increases the generation of hydroxyl radical and peroxynitrite close to the cell nucleus, inflicting DNA damage, but the source of reactive oxygen species (ROS) remains incompletely characterized. We hypothesized that HCV increased the generation of superoxide and H_2O_2 close to the hepatocyte nucleus and that this source of ROS was Nox4. Huh7 human hepatoma cells and telomerase-reconstituted primary human hepatocytes, transfected or infected with virus-producing HCV strains of genotype 2a and 1b, were examined for mRNA, protein, and subcellular localization of Nox proteins, along with human liver. We found that genotype 2a HCV induced persistent elevation of Nox1 and Nox4 mRNA and proteins in Huh7 cells. Genotype 1b HCV likewise elevated the levels of Nox1 and Nox4 in telomerase-reconstituted primary human hepatocytes. Furthermore, Nox1 and Nox4 proteins were increased in HCV-infected human liver compared to uninfected liver. Unlike Nox1, Nox4 was prominent in the nuclear compartment of these cells as well as human liver, particularly in the presence of HCV. HCV-induced ROS and nuclear nitrotyrosine could be decreased with siRNAs to Nox1 and Nox4. Finally, HCV increased the level of transforming growth factor beta-1 (TGFβ1). TGFβ1 could elevate Nox4 expression in the presence of infectious HCV, and HCV increased Nox4 at least in part through TGFβ1.

Conclusion—HCV induced a persistent elevation of Nox1 and Nox4 and increased nuclear localization of Nox4 in hepatocytes *in vitro* and in human liver. Hepatocyte Nox proteins are likely to act as a persistent, endogenous source of ROS during HCV-induced pathogenesis.

Introductory Statement

Hepatitis C virus (HCV) is a blood-borne pathogen that can cause serious liver diseases such as cirrhosis and hepatocellular carcinoma. The mechanism by which HCV induces pathogenesis remains unclear. However, HCV infection is associated with significant oxidative/nitrosative stress with increased lipid peroxidation and oxidative DNA damage,

*Contact Information: Jinah Choi, School of Natural Sciences, University of California, Merced, 5200 N. Lake Rd, Merced, CA 95343. Fax: 209-228-4060. Phone: 209-228-4386. jchoi@ucmerced.edu.

and oxidative/nitrosative stress has been identified as a potential key player in the pathogenesis induced by HCV. In terms of the chemistry, HCV infection has been associated with iron overload, and phlebotomy improves oxidative stress markers and liver pathology, suggesting a role of Fenton chemistry (1). In addition, oxidative DNA damage and mutations to p53 that occur with HCV can be decreased by inhibiting the synthesis of nitric oxide, and nitrotyrosine is elevated in hepatitis C patient liver, indicating that peroxynitrite is also likely to be involved (2). Peroxynitrite is generated in a non-enzymatic reaction between nitric oxide and superoxide anion.

In terms of the source, nitric oxide is likely to derive from inducible nitric oxide synthase, which is induced by HCV. The source of reactive oxygen species (ROS) during HCV infection, however, has not been completely characterized. Several studies have identified mitochondria as the source of ROS in various cell culture models of HCV, and mitochondrial dysfunction is likely to be important in the HCV-induced pathogenesis. However, core protein of the JFH1 strain, which generates infectious virus particles in cell culture, does not localize to the mitochondria, and whether HCV elements are sufficient to induce mitochondrial ROS production, permeability transition, and apoptosis in a consistent manner is unclear (3, 4). In addition, reactive species tend to be compartmentalized in the cell, forming a concentration gradient that originates from their sites of generation (5). In particular, hydroxyl radical is highly reactive and tends to react with whatever molecule is nearby; the chemical reactivity of nitric oxide is also markedly increased by conversion to peroxynitrite. Thus, for HCV to induce peroxynitrite and hydroxyl radical-dependent DNA damage directly, these molecules would need to be generated close to the DNA. Furthermore, unlike nitric oxide and hydrogen peroxide which can diffuse across membranes, whether superoxide anion can escape the mitochondria to react with nitric oxide in the nucleus is questioned. The nitric oxide-dependent nuclear DNA damage that occurs during HCV infection, therefore, suggests that there might be another source of superoxide anion, closer to the cell nucleus.

In this regard, another potential source of ROS during HCV infection are the NAD(P)H oxidase (Nox) proteins which consist of Nox1, 2, 3, 4, 5 and Duox1 and 2 (6). Nox proteins catalyze the transfer of electrons from NAD(P)H to O_2 to produce superoxide and, secondarily, H_2O_2 through dismutation of superoxide. Recently, hepatocytes and Huh7 human hepatoma cells have been found to express Nox family enzymes (7). Furthermore, Nox4 is reported to localize to the nucleus of various cell types (8, 9). Diphenylene iodonium (DPI), which was used to decrease ROS generation by HCV core protein in the initial study by Okuda *et al.*, is also an inhibitor of flavoproteins, commonly used to inhibit Nox (4). There is also a precedent for the activation of Nox2 in phagocytes during HCV infection in response to HCV NS3 protein (1).

The goal of this study, therefore, is to examine the role of hepatocyte Nox protein(s) in ROS and peroxynitrite generation, which is increased by HCV. We hypothesize that HCV increases the generation of peroxynitrite and ROS close to the cell nucleus and that this source of ROS is Nox4. Using state-of-the-art *in vitro* replication models of HCV as well as human liver, we present evidence that: 1) hepatocyte Nox1 and Nox4 are persistently elevated with HCV genotypes 2a and 1b; 2) HCV increases the nuclear localization of Nox4; 3) hepatocyte Nox enzymes are prominent sources of ROS and peroxynitrite generation in the nucleus during HCV infection; and 4) transforming growth factor beta-1 (TGFβ1) is likely to play an important role in the modulation of Nox4 by HCV.

Experimental Procedures

HCV constructs

pJFH1, which generates infectious virus particles of genotype 2a, its replicative-null mutant (pJFH1-GND), subgenomic pSgJFH1-Luc (supports viral RNA genome replication without generating virus particles), and genotype 1b pEF-CG1bRbz/Neo plus its replicative-null mutant (pEF-CG1b GNDRbz/Neo) were used (10, 11).

Cells, transfection/infection, and tissues

Huh7 human hepatoma cells were transfected with *in vitro*-transcribed HCV RNA and cultured, as previously described (12). Telomerase-reconstituted primary human hepatocytes were transfected with pEF-CG1bRbz/Neo, pEF-CG1bGNDRbz/Neo, or control EF-driven vector alone as described for Huh7, and cell clones that are stably transfected with these constructs were selected and maintained in G418-containing medium (Invitrogen) (13). For virus infection, 2 ml of the extracellular medium from JFH1-transfected cells was used to inoculate naïve Huh7 cells with 3 ml of fresh medium, as described (10). Then, the cells were cultured and harvested at various time points, as indicated in Results.

Huh7-Nox4 cells, which constitutively over-express Nox4 enzyme, were generated by transfecting Huh7 cells with human Nox4 cDNA, using lipofectamine 2000 (Invitrogen), and selecting stable cell clones with 0.5 mg/ml G418 (Invitrogen). Control cell clones (Huh7-pcDNA), transfected with empty plasmid vector alone, were also generated. These cells were maintained in 0.25 mg/ml G418-containing medium. For experiments involving these or other stable cell clones, G418 was removed from cell culture medium one day prior to the experiment.

HCV-infected and -uninfected human liver tissues were acquired through the National Disease Research Interchange. Tissues were snap-frozen and were human immunodeficiency virus and hepatitis B virus surface antigen negative. All tissues were from females between ages 49 to 56, from non-liver-related deaths. This study was approved by the Institutional Review Boards at Lawrence Livermore National Laboratory and the University of California, Merced.

Determination of Nox mRNA and protein levels

Total intracellular RNA was extracted using Trizol (Invitrogen). Nox/Duox mRNA levels were quantified by quantitative real time reverse transcriptase-polymerase chain reaction (qRT-PCR), using Power SYBR Green PCR Master Mix. Primer sequences for Nox1, Nox2, Nox3, Nox4, Nox5, Duox1, and Duox2 are summarized in Supplement Table I. Nox4 qRT-PCR results were confirmed by standard RT-PCR, using three different primers sets (Supplement Table I). qRT-PCR reactions without RNA template and without reverse transcriptase served as negative controls. The RNA levels were normalized by 18S rRNA or glyceraldehyde 3-phosphate dehydrogenase (GAPDH) mRNA. Western blot analysis of proteins were carried out, as previously described (12). Data were analyzed by densitometry, using IS2000R (Kodak).

Subcellular fractionation

Subcellular fractionation of nuclear and cytoplasmic fractions was performed as described by Praveen *et al.* (14) or using NE-PER kit (Pierce). Then, the fractions were analyzed by Western blots. Calnexin, *pan*-cadherin, and GAPDH were analyzed as cytoplasmic markers, and lamin A/C and histone deacetylase 1 (HDAC1), as nuclear markers, using antibodies from Santa Cruz Biotechnologies.

Immunofluorescence staining and confocal laser scanning microscopy

Cells were fixed with 3.5 % formaldehyde for 5 min and incubated with phosphate buffered saline, containing 1 (w/v) % bovine serum albumin, 0.05 (w/v) % NaN_3, and 0.02 (w/v) % saponin. Samples were subsequently incubated with primary and then with fluorophore-conjugated secondary antibodies, mounted on microscope slides, and imaged via confocal laser scanning microscopy (C1, Nikon). When propidium iodide (PI) was used, 100 μg/ml RNase A was added during primary antibody incubation to remove the RNA. Tissue samples were fixed for 15 min with 100 % acetone and blocked with 0.4 % triton-X, containing 5 % bovine serum albumin for 30 min prior to incubation with the antibodies.

Small interfering RNA (siRNA)

Control and HCV-replicating cells were transfected with Nox1, Nox4, or non-targeting control siRNAs (100 nM, Smartpool siRNAs, Dharmacon), using RNAiMax (Invitrogen) per manufacturer's protocol.

H_2O_2, superoxide, nitrotyrosine, and Nox enzyme activity measurements

Cells were incubated with 10 μM dihydroethidium (HE) for 30 min and analyzed for intracellular superoxide by monitoring the level of 2-hydroxyethidium (2-OH-E+) by high performance liquid chromatography (HPLC) (15). Extracellular H_2O_2 was measured by horse radish peroxidase-catalyzed p-hydroxyphenylaminoacetic acid dimerization assay (16). Data were normalized by total protein, determined by bicinchoninic acid assay (Pierce). Nitrotyrosine levels were analyzed by confocal microscopy, using antibodies to nitrotyrosine (Santa Cruz Biotechnologies). Total cellular ATP content was determined using ATP Assay Kit (Sigma-Aldrich). Nox enzyme activities were determined by cytochrome c assay (17) (See Supplement for details).

TGFβ1 measurements

TGFβ1 level in the medium samples was determined using TGF-beta 1 Ready-Set-Go! kit (eBioscience) and normalized by cell number.

Statistics

Data were analyzed using Student's t test or one-way analysis of variance, using SigmaStat 3.1 (Jandel Scientific). A p value ≤ 0.05 was considered significant. Data are presented as means ± standard error of the mean. Experiments were repeated 3 – 8 times.

Results

HCV induces pro-oxidative environment with increased levels of ROS

Huh7 human hepatoma cells were transfected with JFH1 RNA of genotype 2a, which generates infectious hepatitis C virus particles in cell culture, and evaluated first for viral replication. Mock-transfection and/or transfection with replicative-null GND RNA were performed as negative controls. Replication of JFH1 but not the GND RNA was readily demonstrated by the continued detection of HCV RNAs and proteins by western blots (Supplement Fig. 1).

To determine whether HCV increased the level of ROS, we measured H_2O_2 concentration. As H_2O_2 diffuses across biomembranes, H_2O_2 concentration was assessed by measuring H_2O_2 extracellularly. As shown in Fig. 1A, H_2O_2 concentration increased significantly with HCV and this increase was almost completely removed by DPI, an inhibitor of flavoproteins. HCV also increased the fluorescence of H_2-dichlorofluorescein diacetate (H_2-

DCF-DA), which measures nonspecific intracellular oxidation, and altered the intracellular glutathione (GSH) concentration in a DPI-sensitive manner (Supplement Fig. 2).

Next, we analyzed the intracellular superoxide concentration by monitoring the generation of 2-OH-E+, a specific product of superoxide, from HE, using HPLC (15). Menadione, which generated ROS via redox cycling, was used as a positive control. Both menadione and HCV increased the level of 2-OH-E+ (Fig. 1B). In contrast, extracellular generation of superoxide, measured by the nitroblue tetrazolium reduction assay, did not increase significantly with HCV ($P > 0.05$; data not shown). Therefore, infectious virus-generating JFH1 strain induced pro-oxidative environment with increased levels of ROS in Huh7 cells.

Nox4 and Nox1 mRNAs are persistently increased with genomic but not subgenomic JFH1 RNA

The data in Fig. 1 also suggested that flavoproteins were involved in the increased generation of ROS in the JFH1 cells. Therefore, we examined whether the mitochondria served as the source of ROS by incubating cells with MitoSOX Red, which measures mitochondrial superoxide, and monitoring its fluorescence by confocal microscopy. Antimycin increased the detection of mitochondrial superoxide anion as expected (Supplement Fig. 2C). However, we did not find any significant increase in the mitochondrial superoxide with JFH1 (Supplement Fig. 2C). In addition, total cellular ATP content was not significantly altered by JFH1 (92.2 ± 4.1 % of control, $P > 0.05$). These data suggested that flavoproteins other than those in the mitochondria were responsible for the increased level of ROS in JFH1-transfected cells.

Next, we evaluated whether hepatocyte Nox proteins played a role in the increased detection of ROS with HCV. Huh7 cells were transfected with JFH1 RNA or mock-transfected and analyzed for Nox mRNA levels by qRT-PCR (7). Cells were also transfected with subgenomic JFH1 RNA for comparison. All seven Nox mRNAs could be detected in these cells (Supplement Table II). Most of all, we found that Nox4 mRNA was significantly elevated in the JFH1 cells, starting at 48 hrs, and the increase persisted at least to day 17 at which point the increase was more than 10 fold (Fig. 2A). In addition, Nox1 mRNA increased significantly with JFH1, and the increase persisted at least to days 14 - 17 (Fig. 2B; also, data not shown). In contrast, Duox2 mRNA increased between 48 to 96 hrs with JFH1 but this increase was not sustained (Fig. 2C). Nox2, Nox3, Nox5, and Duox1 mRNAs did not increase with JFH1 (data not shown). Subgenomic JFH1SgLuc RNA, which supports viral RNA genome replication without producing virus particles, replicated in these cells as expected (Supplement Fig. 3) but did not elevate Nox1, Nox4, or Duox2 mRNAs (Fig. 2C, D). Thus, Nox1 and Nox4 mRNAs showed prolonged elevation with genotype 2a HCV in cell culture, and the structural genes of HCV and/or generation of infectious virions appeared to be necessary for the increases. HCV also increased p22phox, NOXA1, NOXO1, and p67phox mRNAs (Supplement Fig. 4).

Nox4 and Nox1 protein levels are also increased by HCV

Next, Huh7 cells that are either transfected with JFH1 RNA or infected with virus–containing cell culture medium from JFH1 RNA-transfected cells (Supplement Fig. 5) were analyzed for the level of Nox1 and Nox4 proteins by Western blots. Nox1 and Nox4 proteins increased with HCV RNA transfection as well as infection (Fig. 3A, B, D). Higher molecular weight bands (> 65 kDa) were also detected, particularly in the presence of HCV. Furthermore, Nox1 and Nox4 proteins were significantly elevated in HCV-infected human liver compared to uninfected liver (Fig. 3C). Therefore, Nox1 and Nox4 proteins were significantly elevated *in vitro* and during natural infection *in vivo*, in the presence of HCV.

HCV, Nox enzymes, and ROS

To examine whether Nox1 and Nox4 played a role in the virus-induced ROS elevation, we used siRNAs to specifically knockdown Nox1 and Nox4 gene expression in these cells. Nox1 siRNA decreased Nox1 protein level to 27.3 ± 19.2 % of the controls transfected with non-targeting siRNAs, at 72 hrs ($P < 0.05$); Nox4 siRNA decreased Nox4 protein to 45.2 ± 12.3 % of the controls at 72 hrs ($P < 0.05$) (Fig. 4A). In addition, Nox1 and Nox4 siRNAs significantly decreased H_2O_2 and intracellular superoxide concentrations in the JFH1 cells (Fig. 4B and C). Nox1 and Nox4 siRNAs did not decrease other Nox mRNAs and selectively decreased the target protein without affecting Nox4 and Nox1 proteins, respectively (Supplement Fig. 6; also, data not shown). We also performed Nox activity assays using permeabilized Huh7 cells and found increased Nox enzyme activity with HCV that could be inhibited by DPI as well as siRNAs to Nox1 and Nox4 (Fig. 4D). Therefore, Nox1 and Nox4 proteins, which were increased by HCV in these cells, were functionally active in the generation of ROS. Likewise, the HCV-infected liver showed increased NADPH-dependent generation of superoxide that was DPI-sensitive (Fig. 4E).

To examine whether Nox4 over-expression was sufficient to increase the generation of ROS and to ascertain that Nox4 could generate superoxide anion in our system, we also generated Huh7-Nox4 cells that were stably transfected with human Nox4 cDNA. As shown in Fig. 4F, Huh7-Nox4 cells showed increased expression of Nox4 protein compared to the control cell clones, stably transfected with empty plasmid vector instead. Also, both H_2O_2 and intracellular superoxide concentrations were elevated in the Nox4-overexpressing cells (Fig. 4F).

Subcellular localization of Nox1 and Nox4

Next, we determined the subcellular localization of Nox1 and Nox4 proteins by confocal laser scanning microscopy. Nucleus was counter-stained with PI. Nox4 was found in the cytoplasm as well as nucleus in control Huh7 cells (Fig. 5A). In addition, the amount of Nox4 in the nucleus increased significantly with HCV. Conversely, Nox1 showed primarily cytoplasmic, extra-nuclear localization in both control and JFH cells (Fig. 5B). HCV core protein was readily detected in the JFH1 cells, indicating that the viral proteins are being expressed as expected (Fig. 5C). Additional immunofluorescence studies showed a co-localization of Nox4 and calnexin, an ER marker, as well as an overlap between Nox4 and lamin A/C, a nuclear membrane protein; nuclear Nox4 and colocalization of Nox4 with lamin A/C again increased with HCV (Supplement Fig. 7). Cell fractionation studies further confirmed the presence of Nox4 in both cytoplasmic and nuclear fractions from control and JFH1 cells, and the amount of Nox4 protein increased in both fractions with HCV (Fig. 5D). Again, Nox1 was predominantly located in the cytoplasmic fraction, and its location did not change significantly with HCV (Fig. 5E). Therefore, Nox4 showed at least partial nuclear localization in Huh7 cells, and the amount of Nox4 in the nucleus increased with HCV.

Hepatocyte Nox1 and Nox4, genotype 1b HCV, and human liver

The prevalence of genotype 2a HCV can be as high as 20 % depending on the geographical region but the most prevalent genotype is genotype 1. Therefore, we examined whether genotype 1b HCV also increased the nuclear localization of Nox4, using CG1bRbz construct which generates genotype 1b HCV (11). Telomerase-reconstituted primary human fetal hepatocytes that were stably transfected with CG1bRbz/Neo, replicative-null CG1bRbz GND/Neo, or an empty vector alone were selected using G418. Both positive and negative sense HCV RNAs and core protein expression were demonstrated in the CG1bRbz cells by qRT-PCR and immunofluorescence staining (Supplement Fig. 8).

We found that Nox4 protein was increased in CG1bRbz-transfected fetal hepatocytes, compared to cells transfected with CG1bRbz GND or control plasmid alone (Fig. 6A). In addition, Nox4 was prominent in both nucleus and cytoplasm of CG1bRbz-transfected fetal cells (Fig. 6A). Nox1 was also elevated in the hepatocytes with CG1bRbz (Fig. 6B). Genotype 1b subgenomic replicon (Con1), like JFH1 replicon, did not induce Nox1 or Nox4 (data not shown). Therefore, hepatocyte Nox4 and Nox1 were modulated similarly by HCV genotypes 1b and 2a.

Then, we evaluated human liver samples to test whether Nox1 and Nox4 showed similar subcellular localization during natural HCV infection. HCV core protein in the HCV+ liver sample was readily detected by immunofluorescence (Fig. 6C). Consistent with the data in Fig. 3C, increased levels of both Nox1 and Nox4 proteins could be detected in the HCV-infected human liver compared to the uninfected liver (Fig. 6C, D). Furthermore, Nox4 co-localized with lamin A/C in the HCV-infected liver (Fig. 6C). As a control, Duox1 did not increase in these tissues with HCV or show an overlap with lamin A/C (Fig. 6E). Therefore, HCV also increased the nuclear localization of Nox4 during natural HCV infection.

HCV increases the level of nitrotyrosine in nucleus – the role of Nox4

Then, we examined whether Nox4 served as a source of ROS for increased generation of peroxynitrite close to the cell nucleus. Control and HCV-replicating cells were analyzed for nitrotyrosine by confocal microscopy, with and without knocking down Nox1 and Nox4 gene expression with the siRNAs. HCV increased the level of nitrotyrosine in the nucleus (Fig. 7A). In addition, Nox4 siRNA decreased the level of nitrotyrosine in the nucleus as did N^G-methyl-L-arginine acetate (L-NMA), an inhibitor of nitric oxide synthase (Fig. 7B). Nox1 siRNA also led to an overall decrease in the level of nitrotyrosine in these cells but, unlike Nox4 siRNA, some nuclear nitrotyrosine remained (see the arrows, Fig. 7B). In addition, we performed Nox activity assay using nuclear fractions from JFH1 and mock-transfected cells, and found increased generation of superoxide with HCV that was DPI-sensitive (Fig. 7C); nuclear Nox activity could also be partly attenuated with Nox4 siRNA by 24.7 ± 1.3 % ($P < 0.05$). Therefore, hepatocyte Nox enzymes could act as a prominent source of ROS for the generation of peroxynitrite in and around the nucleus during complete HCV replication.

TGFβ1 is involved in the elevation of Nox4 by HCV

TGFβ has been shown to induce Nox4, and TGFβ concentration is elevated in hepatitis C patients (6, 18). Thus, we evaluated whether HCV increased the level of TGFβ in our system and whether HCV elevated Nox4 through TGFβ. TGFβ1 increased Nox4 mRNA in the HCV-replicating cells (Fig. 8A). Furthermore, HCV increased the level of TGFβ1, and HCV-induced increase in Nox4 could be attenuated using antibodies to TGFβ1 (Fig. 8B, C). These data suggest that TGFβ1 is involved in the elevation of Nox4 by HCV.

Discussion

Oxidative/nitrosative stress has been increasingly implicated in viral infections, including HCV, but the sources of ROS during HCV infection have not been completely characterized. Here, using state-of-the-art HCV cell culture systems and human liver samples, we present evidence that hepatocyte Nox1 and Nox4 are prominent sources of ROS during complete HCV replication. In agreement with a recent report that JFH1 core does not localize to the mitochondria, we did not find a significant elevation of mitochondrial ROS or ATP depletion with JFH1 (3). However, it is possible that the role of the mitochondria in the HCV-induced oxidative stress is more pronounced with certain viral genotypes or cell types. Previously, HCV core protein was suggested to reduce the cell's ability to upregulate its

antioxidant defenses (1). However, hepatitis C patients have elevated levels of antioxidant genes, and JFH1 increased GSH concentration in our study (Supplement Fig. 2B) (1); thus, to what extent HCV interferes with the antioxidant defense mechanisms during complete viral replication remains to be further examined.

In this study, our objective was not only to find a source of ROS during complete HCV replication but to find the source of superoxide for peroxynitrite generation which we predicted would occur near the cell nucleus. Consistent with this hypothesis, nitrotyrosine and Nox activity were increased in the JFH1-transfected cell nucleus, and this increase was attenuated with siRNAs to Nox. Also, although the relative amount of nuclear vs. cytoplasmic Nox4 tended to vary from one experiment to another, Nox4 was always at least partly nuclear and colocalized with lamin A/C, particularly in the presence of HCV. Furthermore, HCV elevated intracellular superoxide concentration, and Huh7 cells overexpressing Nox4 showed increased superoxide level. These data do not completely rule out the possibility that Nox4 generates superoxide indirectly through other source(s) of superoxide in the cell, and the significant effect that Nox1 siRNA had on nuclear nitrotyrosine could at least in part be due to the uncoupling of nitric oxide synthase by peroxynitrite. Nevertheless, our data strongly indicate that Nox enzymes can elevate intracellular superoxide concentration either directly or indirectly in the cell, leading to increased generation of peroxynitrite in the hepatocyte nucleus during HCV infection. Indeed, although Nox4 has recently been suggested to generate H_2O_2 rather than superoxide, by the virtue of their chemical mechanism involving a terminal electron transfer from the one-electron carrying heme B, Nox family proteins must generate superoxide first, prior to formation of secondary products (6). Thus, reported inability to detect superoxide with some Nox/Duox enzymes is likely to be due to rapid dismutation of superoxide to form H_2O_2, which under some circumstances occurs more rapidly than the reaction with superoxide detecting probe. Also, if anything can outcompete superoxide dismutase (SOD) for superoxide, it will be nitric oxide reacting with superoxide to generate peroxynitrite (5). In fact, we were able to detect higher amount of 2-OH-E+ by inhibiting SOD in our cells, suggesting a significant competition between the probe and SOD for reacting with superoxide (unpublished observation). ROS/RNS thus generated would then cooperate with other Nox/Duox enzymes and other potential sources of ROS outside nucleus to induce a chronic state of oxidative/nitrosative stress during HCV infection. In this scheme, ROS generated by nuclear Nox4 and other extra-nuclear sources of ROS would form concentration gradients, the probability of their reacting with target molecules diminishing with increasing distance from their respective origin (Fig. 8D).

Our discovery of nuclear Nox4 raises questions as to exactly where in the nucleus Nox4 is located and how HCV changes the location of Nox4 without affecting the location of Nox1. Nox family enzymes have multiple transmembrane domains and are membrane-bound (6). In this regard, it may be important to note that the ER membrane is contiguous with the nuclear membrane. Also, the nucleoplasm is generally membrane free but intranuclear membrane structures have been reported (19), and Nox4 might be located within the inner or outer nuclear membrane or intranuclear cisternae of hepatocytes. If Nox4 is responsible for peroxynitrite-dependent DNA damage, it is most likely be located on the inner nuclear membrane or intranuclear membrane, with its active site facing the nucleoplasm. Notice that in our nuclear Nox activity assays, the nuclear pore is likely to allow NADPH, cytochrome c, and SOD to enter the nucleus. Detailed analysis of the subcellular location of Nox4 by electron microscopy is underway. In regards to the mechanism of increased nuclear localization of Nox4, HCV is known to induce severe membrane and nuclear alterations (20). Thus, increased nuclear location of Nox4 might be a consequence of virus modifying the cell for its replication. In addition, as some Nox4 could be found in the nucleus even without HCV (Fig. 5), nuclear Nox4 is likely to represent a normal cellular process that is

enhanced by HCV. In this study, we focused primarily on 50 to 65 kDa Nox1/4 protein bands which corresponded to the expected sizes of Nox1 and Nox4 proteins. The higher molecular weight bands, however, also increased with HCV and could be partly decreased with siRNAs (Fig. 3 and 4), and might represent Nox protein complexes or post-translationally modified Nox (9).

Nox enzymes are implicated in anti-microbial defense, toll-like receptor signaling, lung fibrosis, and cancers. H_2O_2 and Nox enzymes can also increase iron uptake and mediate many biological effects of TGFβ (14). Tumor necrosis factor alpha and TGFβ, which are pro-inflammatory and fibrogenic cytokines, are elevated during HCV infection, and these cytokines are known inducers of Nox4 (6, 18). We also found that TGFβ played a major role in the HCV-induced elevation of Nox4 in hepatocytes, although other factors might also be involved (Fig. 8; also, unpublished findings). Some of these findings were corroborated by a recent study by Boudreau *et al.* (21). Importantly, hepatocellular carcinoma, associated with chronic hepatitis C, is typically preceded by cirrhosis. Therefore, hepatocyte Nox protein(s) may provide a link between inflammation, fibrogenesis, and hepatocarcinogenesis during chronic hepatitis C. In particular, nuclear Nox4 is likely to be highly significant in the HCV-induced DNA damage in the initiation of cancer as well as reversible and/or irreversible protein modifications in the modulation of cell signaling and host gene expression. The ability to regulate Nox proteins also makes them potential targets for therapy. Therefore, our study provides new insights into possible mechanism of HCV-induced pathogenesis and points to potential targets for therapy, directed at the source of ROS.

Supplementary Material

Refer to Web version on PubMed Central for supplementary material.

Acknowledgments

References

1. Seronello S, Sheikh MY, Choi J. Redox regulation of hepatitis C in nonalcoholic and alcoholic liver. Free Radic Biol Med. 2007; 43:869–882. [PubMed: 17697932]

2. Garcia-Monzon C, Majano PL, Zubia I, Sanz P, Apolinario A, Moreno-Otero R. Intrahepatic accumulation of nitrotyrosine in chronic viral hepatitis is associated with histological severity of liver disease. J Hepatol. 2000; 32:331–338. [PubMed: 10707875]

3. Rouille Y, Helle F, Delgrange D, Roingeard P, Voisset C, Blanchard E, Belouzard S, et al. Subcellular localization of hepatitis C virus structural proteins in a cell culture system that efficiently replicates the virus. J Virol. 2006; 80:2832–2841. [PubMed: 16501092]

4. Okuda M, Li K, Beard MR, Showalter LA, Scholle F, Lemon SM, Weinman SA. Mitochondrial injury, oxidative stress, and antioxidant gene expression are induced by hepatitis C virus core protein. Gastroenterology. 2002; 122:366–375. [PubMed: 11832451]

5. Beckman JS, Koppenol WH. Nitric oxide, superoxide, and peroxynitrite: the good, the bad, and ugly. Am J Physiol. 1996; 271:C1424–1437. [PubMed: 8944624]

6. Lambeth JD, Kawahara T, Diebold B. Regulation of Nox and Duox enzymatic activity and expression. Free Radic Biol Med. 2007; 43:319–331. [PubMed: 17602947]

7. Reinehr R, Becker S, Keitel V, Eberle A, Grether-Beck S, Haussinger D. Bile salt-induced apoptosis involves NADPH oxidase isoform activation. Gastroenterology. 2005; 129:2009–2031. [PubMed: 16344068]

8. Ushio-Fukai M. Compartmentalization of redox signaling through NADPH oxidase-derived ROS. Antioxid Redox Signal. 2009; 11:1289–1299. [PubMed: 18999986]

9. Hilenski LL, Clempus RE, Quinn MT, Lambeth JD, Griendling KK. Distinct subcellular localizations of Nox1 and Nox4 in vascular smooth muscle cells. Arterioscler Thromb Vasc Biol. 2004; 24:677–683. [PubMed: 14670934]

10. Wakita T, Pietschmann T, Kato T, Date T, Miyamoto M, Zhao Z, Murthy K, et al. Production of infectious hepatitis C virus in tissue culture from a cloned viral genome. Nat Med. 2005; 11:791–796. [PubMed: 15951748]

11. Heller T, Saito S, Auerbach J, Williams T, Moreen TR, Jazwinski A, Cruz B, et al. An in vitro model of hepatitis C virion production. Proc Natl Acad Sci U S A. 2005; 102:2579–2583. [PubMed: 15701697]

12. Choi J, Lee KJ, Zheng Y, Yamaga AK, Lai MMC, Ou JH. Reactive oxygen species suppress hepatitis C virus RNA replication in human hepatoma cells. Hepatology. 2004; 39:81–89. [PubMed: 14752826]

13. Wege H, Le HT, Chui MS, Liu L, Wu J, Giri R, Malhi H, et al. Telomerase reconstitution immortalizes human fetal hepatocytes without disrupting their differentiation potential. Gastroenterology. 2003; 124:432–444. [PubMed: 12557149]

14. Vayalil PK, Iles KE, Choi J, Yi AK, Postlethwait EM, Liu RM. Glutathione suppresses TGF-beta-induced PAI-1 expression by inhibiting p38 and JNK MAPK and the binding of AP-1, SP-1, and Smad to the PAI-1 promoter. Am J Physiol Lung Cell Mol Physiol. 2007; 293:L1281–1292. [PubMed: 17890327]

15. Zielonka J, Vasquez-Vivar J, Kalyanaraman B. Detection of 2-hydroxyethidium in cellular systems: a unique marker product of superoxide and hydroethidine. Nat Protoc. 2008; 3:8–21. [PubMed: 18193017]

16. Liu RM, Gao L, Choi J, Forman HJ. gamma-glutamylcysteine synthetase: mRNA stabilization and independent subunit transcription by 4-hydroxy-2-nonenal. Am J Physiol. 1998; 275:L861–869. [PubMed: 9815102]

17. Li JM, Mullen AM, Yun S, Wientjes F, Brouns GY, Thrasher AJ, Shah AM. Essential role of the NADPH oxidase subunit p47(phox) in endothelial cell superoxide production in response to phorbol ester and tumor necrosis factor-alpha. Circ Res. 2002; 90:143–150. [PubMed: 11834706]

18. Nelson DR, Gonzalez-Peralta RP, Qian K, Xu Y, Marousis CG, Davis GL, Lau JY. Transforming growth factor-beta 1 in chronic hepatitis C. J Viral Hepat. 1997; 4:29–35. [PubMed: 9031062]

19. Isaac C, Pollard JW, Meier UT. Intranuclear endoplasmic reticulum induced by Nopp140 mimics the nucleolar channel system of human endometrium. J Cell Sci. 2001; 114:4253–4264. [PubMed: 11739657]

20. Naas T, Ghorbani M, Alvarez-Maya I, Lapner M, Kothary R, De Repentigny Y, Gomes S, et al. Characterization of liver histopathology in a transgenic mouse model expressing genotype 1a hepatitis C virus core and envelope proteins 1 and 2. J Gen Virol. 2005; 86:2185–2196. [PubMed: 16033966]

21. Boudreau HE, Emerson SU, Korzeniowska A, Jendrysik MA, Leto TL. Hepatitis C virus (HCV) proteins induce NADPH oxidase 4 expression in a transforming growth factor beta-dependent manner: a new contributor to HCV-induced oxidative stress. J Virol. 2009; 83:12934–12946. [PubMed: 19812163]

List of Abbreviations

HCV   hepatitis C virus

ROS   reactive oxygen species

Nox	NAD(P)H oxidase
DPI	diphenylene iodonium
qRT-PCR	quantitative reverse transcriptase-polymerase chain reaction
GAPDH	glyceraldehyde 3-phosphate dehydrogenase
HDAC1	histone deacetylase 1
PI	propidium iodide
siRNA	small interfering RNA
HE	dihydroethidium
2-OH-E+	2-hydroxyethidium
HPLC	high performance liquid chromatography
TGFβ1	transforming growth factor beta 1
DCF-DA	H_2-dichlorofluorescein diacetate
GSH	glutathione
L-NMA	N^G-methyl-L-arginine acetate
SOD	superoxide dismutase

(A)

(B)
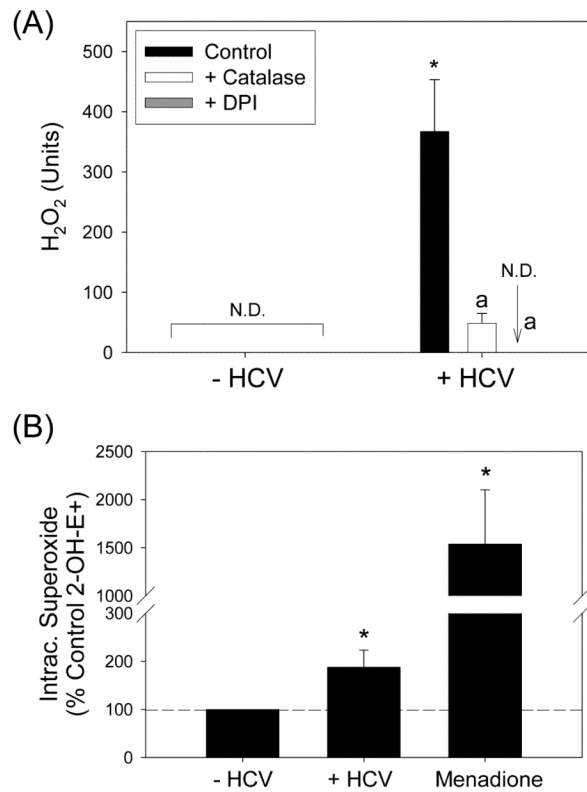
Fig. 1. HCV increases the level of ROS

Huh7 cells transfected with virus-producing JFH1 HCV RNA or mock-transfected were analyzed for H_2O_2 by p-hydroxyphenylaminoacetic acid dimerization assay (A) and intracellular superoxide by measuring 2-OH-E+ by HPLC (B). Menadione (50 μM) plus diethyldithiocarbamate (3 mM, inhibitor of superoxide dismutase; added 30 min prior to HE) served as the positive control for the detection of 2-OH-E+ (B). When used, DPI was added at 10 μM concentration 30 min prior to the assays. Catalase was added at the final concentration of 200 U/ml. Data were normalized by total protein. *, [a] indicate statistically significant difference from HCV− or HCV+ controls, respectively ($P < 0.05$); N.D. indicates "non-detectable" (below baseline).
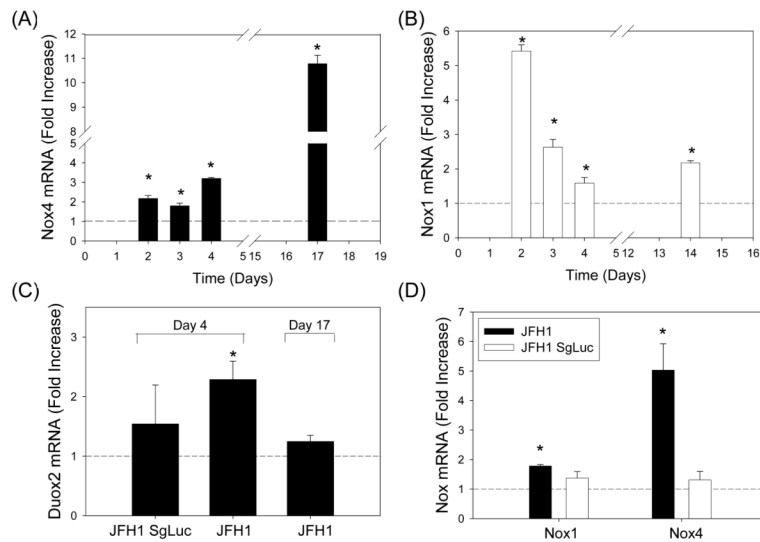
Fig. 2. Differential expression of Hepatocyte Nox mRNAs in Huh7 cells generating infectious HCV
Huh7 cells were transfected with virus-producing full-length JFH1 RNA, non-virus-producing subgenomic JFH1 RNA, or mock-transfected (control) and analyzed for Nox4 (A, D), Nox1 (B, D), and Duox2 (C) mRNAs by qRT-PCR. Data were calculated and normalized by 18S rRNA or GAPDH mRNA by ΔΔCt method and expressed as fold increase from the controls. * indicates statistically significant difference from the controls (P < 0.05).
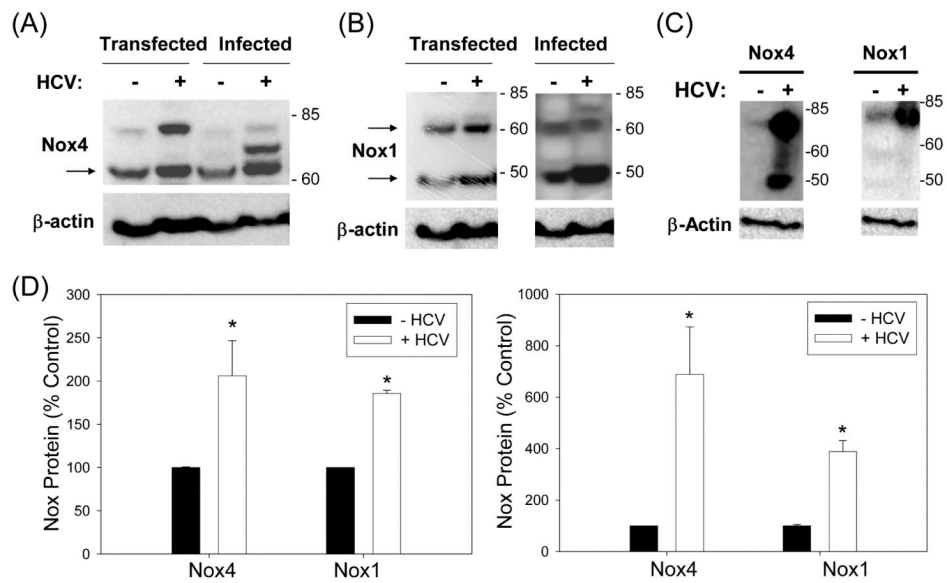
Fig. 3. Hepatocyte Nox1 and Nox4 proteins are increased with HCV

Huh7 cells were transfected with virus-producing full-length JFH1 RNA or mock-transfected, or infected with medium from the HCV RNA and GND RNA-transfected cells, and analyzed for Nox4 (A) and Nox1 (B) protein levels by western blots. Human liver samples from HCV-infected and non-infected donors (National Disease Research Exchange, NDRI) were also analyzed for Nox1 and Nox4 proteins by western blots (C). β-actin was analyzed as loading control. (D) Nox1 (50 kDa) and Nox4 (65 kDa) protein levels in control and JFH1 cells (left panel), and Nox1 and Nox4 proteins (> 60 kDa) in human liver tissues (right panel) were quantified by densitometry and normalized by the level of β-actin. * indicates statistically significant difference from the controls (P < 0.05). Arrows indicate expected sizes of Nox1 and Nox4.
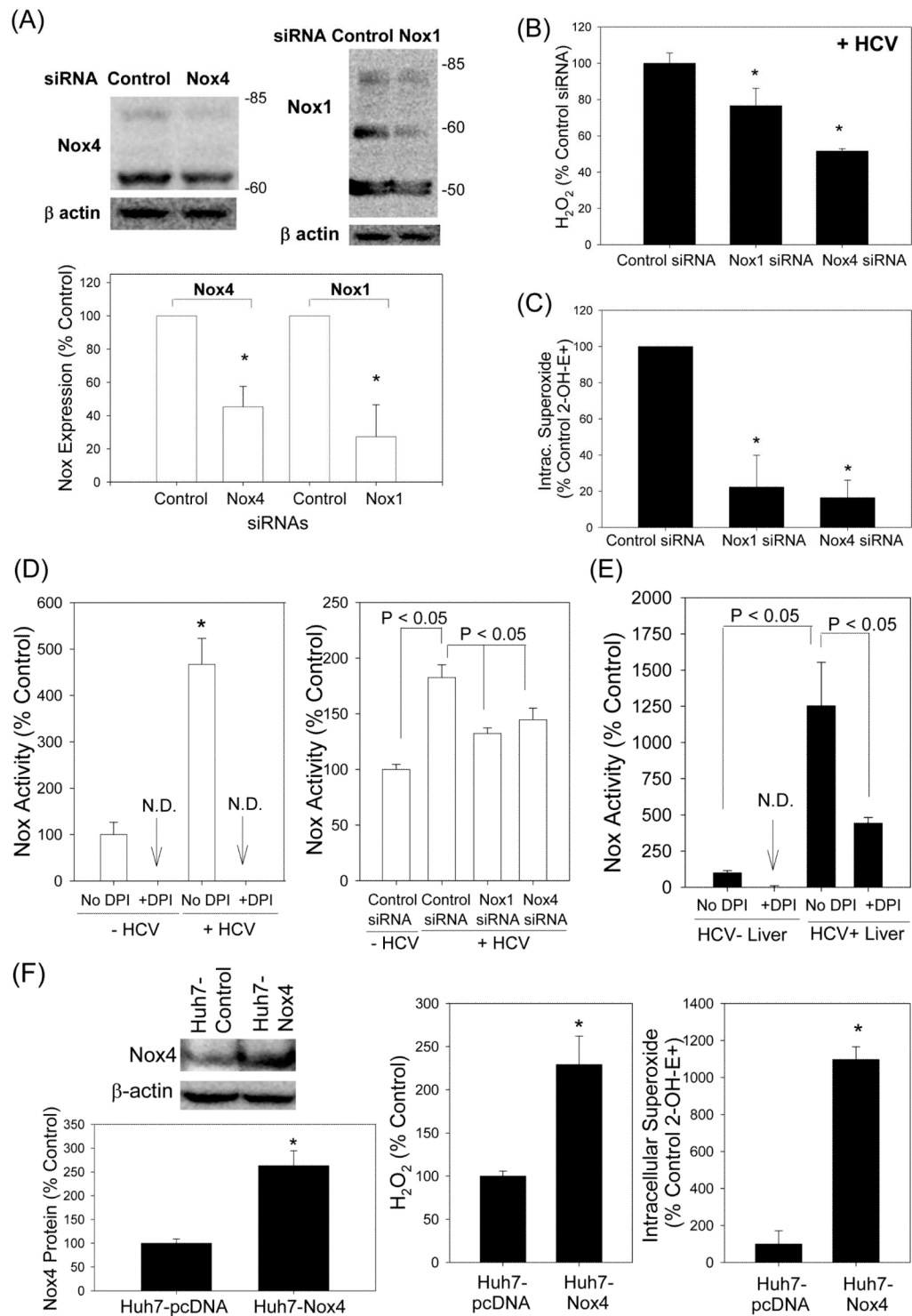
Fig. 4. Role of Nox enzymes in HCV-induced ROS
(A – C) Twenty four hrs after JFH1 RNA transfection, Huh7 cells were transfected with non-targeting control siRNA, Nox1 siRNA, or Nox4 siRNA and, after another 72 hrs, analyzed for the level of Nox1 and Nox4 proteins by western blots (A), H_2O_2 by p-hydroxyphenylaminoacetic acid dimerization assay (B), and intracellular superoxide by

measuring 2-OH-E+ via HPLC (C). (D) Cells were permeabilized with intracellular-like buffer containing 40 μM digitonin, and Nox enzyme activities were determined by monitoring NADPH-dependent and SOD-inhibited reduction of cytochrome c, in the presence and absence of 30 μM DPI, as described in the Supplement. Activity assays were also carried out after transfecting cells with non-targeting control siRNA, Nox1 siRNA, or Nox4 siRNA. (E) Human liver samples were sonicated in intracellular-like buffer, and SOD-inhibited reduction of cytochrome c was determined in the presence and absence of DPI, as described in the Supplement. (F) Huh7 cells stably transfected with Nox4 cDNA or empty plasmid vector (pcDNA) alone were analyzed for Nox4 protein, H_2O_2, and superoxide, as described. Nox proteins were quantified by densitometry and normalized by β-actin. Data in (B - F) were normalized by total protein. * indicates statistically significant difference from controls ($P < 0.05$). N.D. indicates "non-detectable" (below baseline).
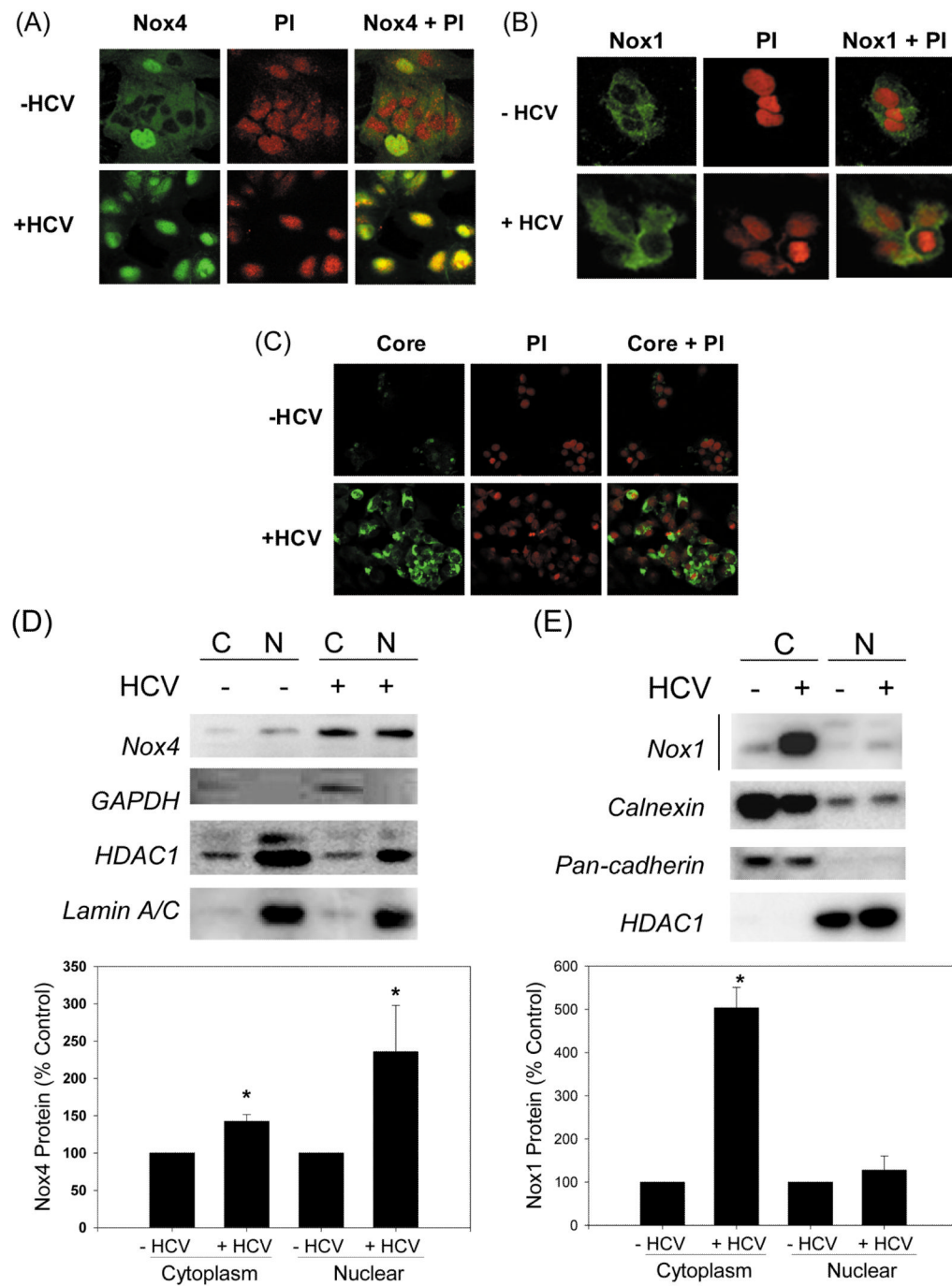
Fig. 5. Subcellular localization of Nox1 and Nox4 enzymes in control vs. HCV-replicating cells
(A – C) Huh7 cells transfected with JFH1 HCV RNA and mock-transfected control cells were analyzed for subcellular location of Nox1 (A), Nox4 (B), and HCV core (C) proteins by confocal microscopy. Nucleus was counter stained with PI in (A – C). (D - E) Control and JFH1-transfected Huh7 cells were fractionated and analyzed for Nox1 and Nox4 proteins by western blots. Samples were also analyzed for cytoplasmic (GAPDH, calnexin, cadherin) and nuclear (HDAC1, lamin A/C) markers. Nox1 and Nox4 protein bands were quantified by densitometry, and normalized by HDAC1 or calnexin for nuclear and

cytoplasmic fractions, respectively. C indicates cytoplasmic fraction; N indicates nuclear fraction. * indicates statistically significant difference from the controls (P < 0.05).
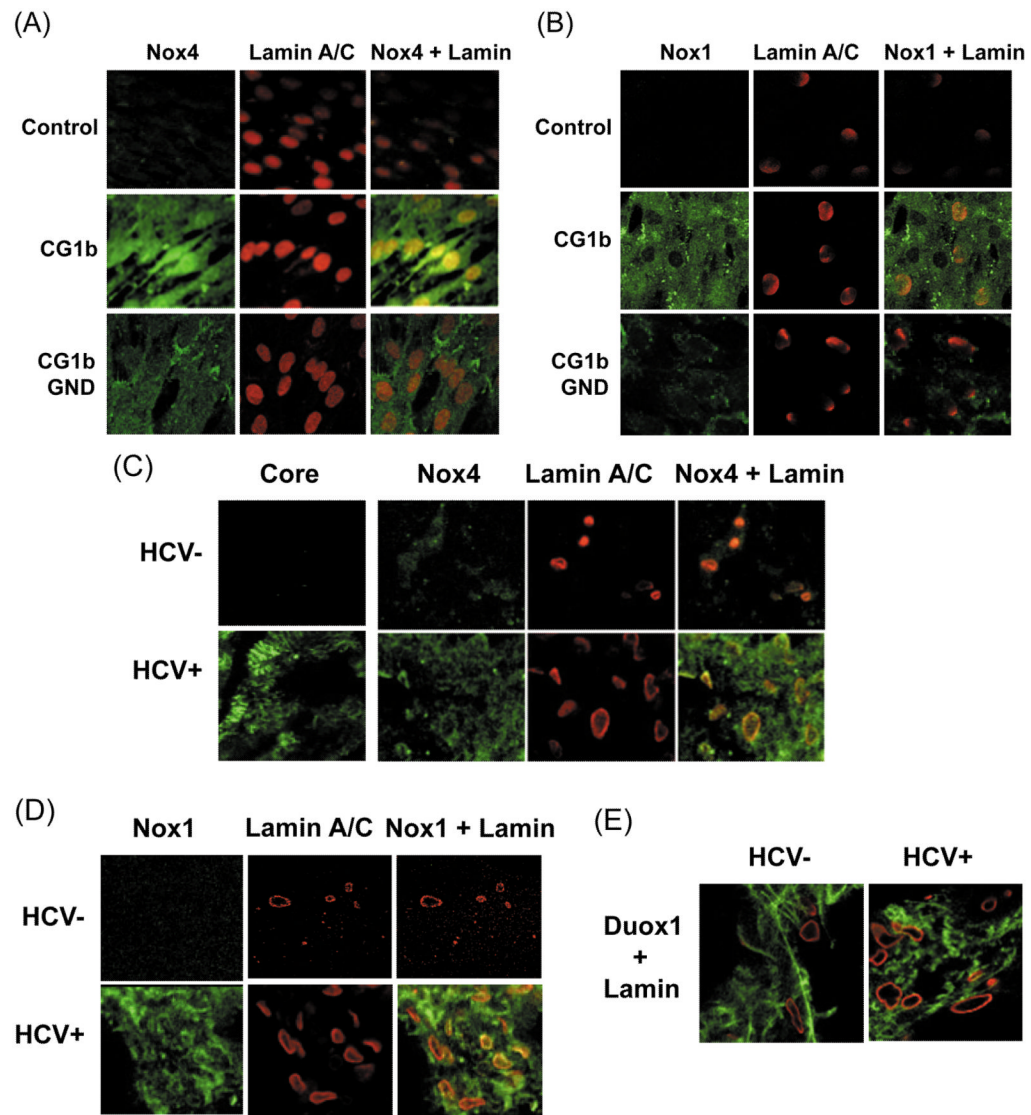
Fig. 6. Hepatocyte Nox1 and Nox4 in genotype 1b HCV-replicating cells and human liver
(A – B) Telomerase-reconstituted primary human hepatocytes, stably transfected with pEF-CG1bRbz/Neo, pEF-CG1bRbz GND/Neo, or control vector alone, were analyzed for Nox4 (A) and Nox1 proteins (B) by confocal microscopy. Lamin A/C was also analyzed as a nuclear marker. (C – E) HCV-infected (HCV+) and un-infected (HCV-) human liver samples were analyzed for Nox4 (C), Nox1 (D), and Duox1 (E) proteins by immunofluorescence, using confocal microscopy. Nuclear membrane was stained with lamin A/C. Nox/Duox proteins are shown in green and lamin A/C, in red in (C – E).
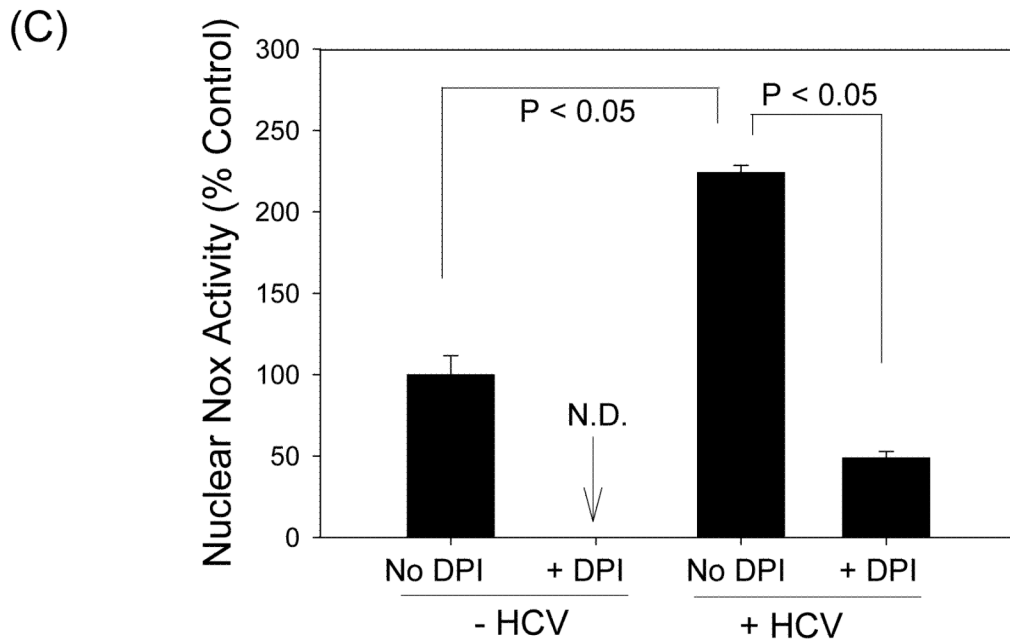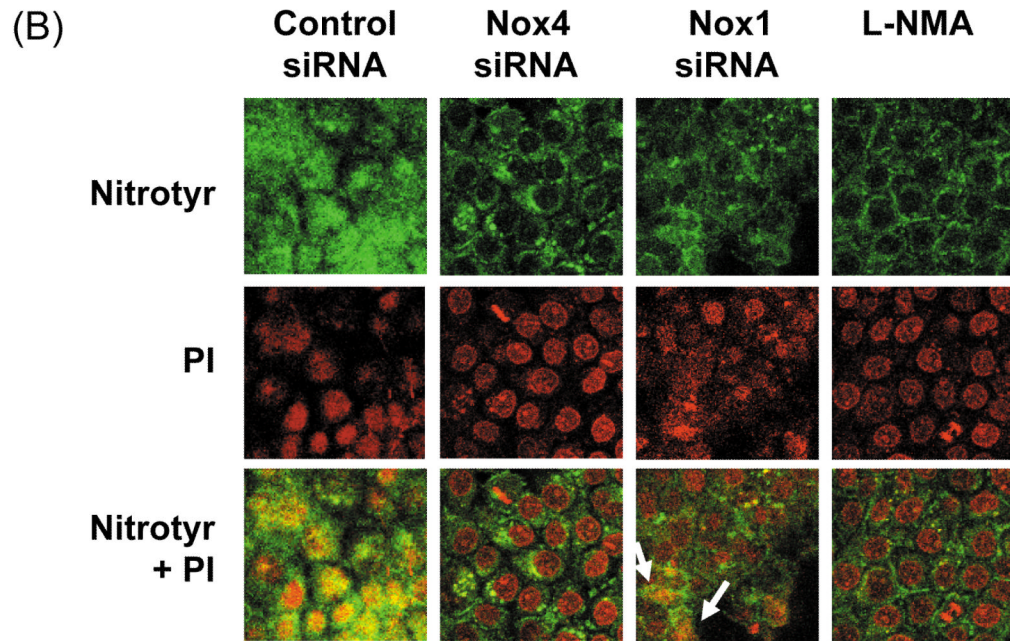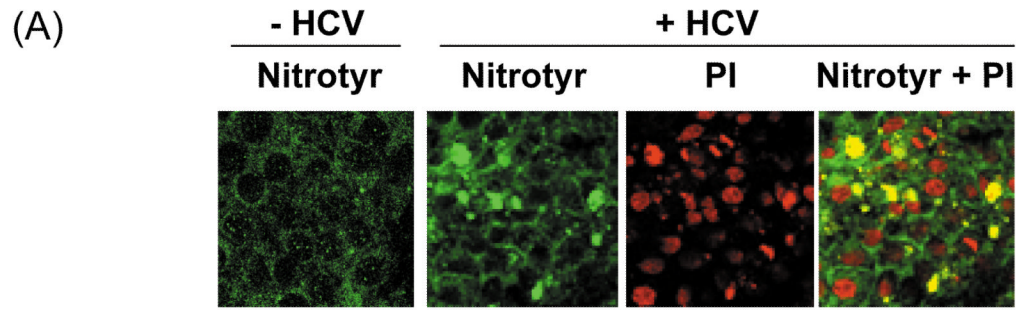
Fig. 7. HCV, Nox enzymes, and nitrotyrosine
(A) Nitrotyrosine in control and JFH1 cells was analyzed by immunofluorescence via confocal microscopy. (B) JFH1 transfected cells were transfected with control, Nox1, or Nox4 siRNAs, or transfected with control siRNA and treated with 1 mM L-NMA. Then, the samples were analyzed for nitrotyrosine, as described. Nucleus was counter-stained with PI. (C) Nuclear fractions were isolated from JFH1 and mock-transfected cells as described in the Experimental Procedures, and Nox activity was analyzed by monitoring NADPH-dependent and SOD-inhibited reduction of cytochrome c, in the presence and absence of 30 μM DPI. N.D. indicates "non-detectable" (below baseline).
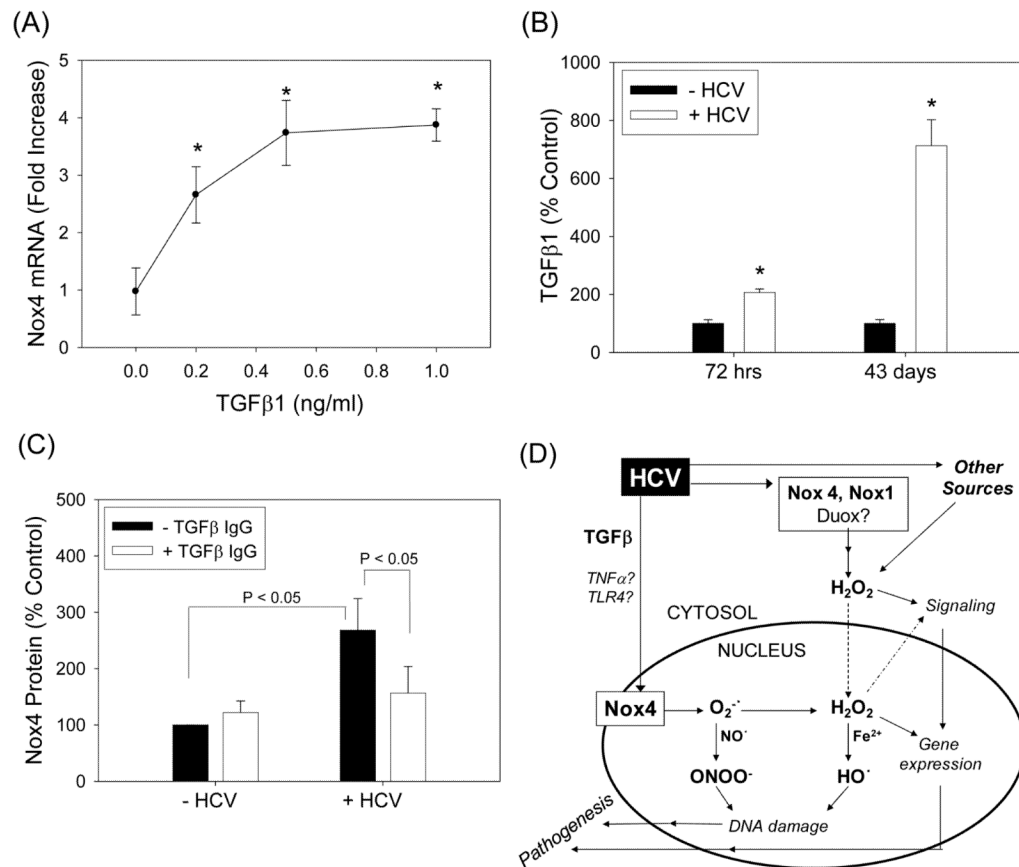
Fig. 8. Role of TGFβ in the modulation of Nox4 by HCV
(A) Huh7 cells transfected with JFH1 RNA were cultured with heat-inactivated serum overnight, serum-starved for 24 hrs, and treated with indicated concentrations of recombinant human TGFβ1 (R&D Systems) daily for another 72 hrs. Then, samples were analyzed for Nox4 mRNA by qPCR. Data were normalized by GAPDH mRNA content. (B) Cell culture medium from control and JFH1 cells were analyzed for TGFβ1 concentration. Data were normalized by cell number and expressed as percentage of controls, where control values were $2{,}133.5 \pm 277.9$ and $2{,}720.8 \pm 359.6$ pg per 10^6 cells at 72 hrs and 43 days, respectively. TGFβ1 present in the cell culture serum was subtracted from the readings. (C) Control and JFH1 cells were incubated with 2 μg/ml of anti-TGFβ1 antibodies (R&D Systems) and, after 48 or 72 hrs, analyzed for Nox4 protein concentration by Western blots. Nox4 protein was quantified by densitometry and normalized by the level of β-actin. * indicates statistically significant difference from controls ($P < 0.05$). (D) Proposed role of hepatocyte Nox proteins in HCV-induced pathogenesis.